

## Automatic blood vessel detection using fractional Hessian matrices

### Detección automática de vasos sanguíneos usando matrices Hessianas fraccionarias

MARTÍNEZ-JIMÉNEZ, Leonardo<sup>†\*</sup>, LÓPEZ-LARA, Pedro, FLORES-BALDERAS, Adán and LÓPEZ-HERNÁNDEZ, Juan Manuel

*Universidad de Guanajuato, Departamento de Estudios Multidisciplinarios, División de Ingenierías, Campus Irapuato-Salamanca, Av. Universidad S/N, Col. Yacatitas Yuriria Gto., , C.P. 38940. México.*

ID 1<sup>st</sup> Author: *Leonardo, Martínez-Jiménez* / ORC ID: 0000-0002-7062-7154, CVU CONACYT ID: 165253

ID 1<sup>st</sup> Co-author: *Pedro, López-Lara* / ORC ID: 0000-0000-7908-3280

ID 2<sup>nd</sup> Co-author: *Adán, Flores-Balderas* / ORC ID: 0000-0002-1789-8393

ID 3<sup>rd</sup> Co-author: *Juan Manuel, López-Hernández* / ORC ID: 0000-0001-6546-4357

DOI: 10.35429/EJT.2022.11.6.12.19

Received January 20, 2022; Accepted June 30, 2022

#### Abstract

The enhancement of blood vessels is a vital stage in imaging. The goal of this project is to improve the evaluation of the performance of a method for enhancing arteries in coronary angiograms, which use fractional derivatives. In this work an algorithm for automatic enhancement of vessels in coronary angiograms is evaluated, the method uses the Hessian matrix, the eigenvalues and the Grünwald-Letnikov fractional derivative with fractional order  $\omega$  in the interval (1,3). The probes of the performance of the method were made using a set of 20 coronary angiograms with its respective ground-truth image and the area under the ROC's curve. The fractional orders are  $2 < \omega$  and the second interval  $2 \geq \omega$ . The results show that the maximum values of area under the ROC's curve are obtained when the derivative order is in the interval  $2 < \omega < 2.15$ .

**Evaluation, Coronary, Hessian matrix, Derivatives**

#### Resumen

El realzado de vasos sanguíneos es una etapa vital en tareas de segmentación de imágenes médicas. El objetivo de este proyecto es mejorar la evaluación del desempeño de un algoritmo para realzado de arterias en angiogramas de coronarias que utiliza derivadas fraccionarias. En este trabajo se evalúa un método para realzado de vasos sanguíneos que utiliza la matriz Hessiana, los eigenvalores y la derivada Grünwald-Letnikov con ordenes fraccionarios  $\omega$  en el intervalo (1,3). La evaluación del desempeño del realzador de angiogramas de orden fraccionario se realizó utilizando un conjunto de 20 imágenes de angiogramas de coronarias con su respectiva imagen ground-truth y el área bajo la curva ROC como parámetro de medición. Para las pruebas se usaron los intervalos de  $2 < \omega$  y  $2 \geq \omega$  de ordenes fraccionarios. Las pruebas muestran que se obtienen los mejores resultados cuando se utilizan ordenes de derivadas,  $2 < \omega < 2.15$ .

**Evaluación, Coronarias, Matriz Hessiana, Derivadas**

**Citation:** MARTÍNEZ-JIMÉNEZ, Leonardo, LÓPEZ-LARA, Pedro, FLORES-BALDERAS, Adán and LÓPEZ-HERNÁNDEZ, Juan Manuel. Automatic blood vessel detection using fractional Hessian matrices. ECORFAN Journal-Taiwan. 2022. 6-11:12-19.

\* Correspondence to Author (E-mail: leonardomj@ugto.mx)

† Researcher contributing as first author.

## Introduction

The arteries are the most muscular, elastic vessels and carry blood from the heart to the arterioles. From here the blood enters the capillaries, the narrowest vessels, where all exchanges between blood and tissues take place, (Guzmán *et al.* 2022). That is why its correct operation is very important. An early diagnosis in arteries and the heart can help prevent irreversible damage, (Navarrete Chiriboga and Rivera Guerra 2022).

Enhance of vessels is a basic step in the segmentation process of medical images for Computer-Assisted Diagnosis (CAD). The target of the enhancement is improving the quality of the images to apply algorithms for diagnosis. To upgrade medical images like the angiograms, some algorithms have been proposed: some of them are based on morphological operations (Bouraoui *et al.* 2008), (Eiho and Qian 1997), (Lara *et al.* 2009), (Maglaveras *et al.* 2001). The others are based on the properties of the Hessian matrix (Kang *et al.* 2009) and (Frangi *et al.* 1998). In 2015 a segmentation method which works on two steps: first the structure of the vessels is detected using the properties of the Hessian matrix, after, an evolutive algorithm is utilized in thresholding tasks (Cruz-Aceves *et al.* 2015) and, in (Angeles Rojas, 2022) a method for detecting basal cell carcinoma using convolutional neural network and Support Vector Machine is described in (Angeles Rojas, 2022).

On the other hand, the Fractional Calculus (FC) is an extension of the traditional calculus and is devoted to integrals and derivatives of non-integer order. It is based on the properties of some special functions like the gamma function. Through the years, the FC has been transformed, and some different definitions of integrals and derivatives have been appeared. The first definitions were Riemann-Liouville integral and derivative, the Grünwald-Letnikov (GL) derivative (Capelas de Oliveira and Tenreiro Machado 2014), the Caputo fractional derivative (Caputo and Mainardi 1971), the Caputo-Fabrizio fractional derivative (Caputo *et al.* 2015), the Atangana-Baleanu definition (Atangana *et al.* 2016) and the Conformable derivative (Khalil *et al.* 2014), among others.

In the last years the FC has suffered a strong growth, due to practical applications in many knowledge fields. The first application was implemented by Abel solving the problem of the tautochrone curve (Abel 2012a), (Abel 2012b), since the number of applications has increased exponentially. Today the FC is utilized in fields like dynamic (Ahmad B. *et al.* 2015), viscoelastic models (Schiesselt *et al.* 1995) and (Meral *et al.* 2010), anomalous diffusion (Chen *et al.* 2010), electrical circuits (Ahmed *et al.* 2015) and (Guía *et al.* 2013), catenary based curves (Martinez-Jimenez *et al.* 2019), economic models (Baskonus *et al.* 2015), modelling of the movements of the electrons in conductive materials (Martinez-Jimenez L. *et al.* 2017) and (Karpinski *et al.* 2021), image processing (Amoako-Yirenkyi *et al.* 2016).

The mission of this work is refining the obtained results on (Martinez-Jimenez *et al.* 2018), using a more robust image base and comparing results with fractional orders in the interval  $1.0 < \omega < 3.0$ . The used base of images is composed by 20 coronary angiograms of  $300 \times 300$  pixels, each image has a corresponding ground-truth image, which were generated by a specialist of the Instituto Mexicano del Seguro Social UMAE T1 León, (Cervantes-Sanchez *et al.* 2019).

The conformation of this work is as follows: in the next section the Hessian matrix and the GL fractional derivative are described, also, the Hessian matrix based method of Frangi is described. Following, the proposed method with the GL fractional derivatives to enhance angiograms is presented, after the results are evaluated using the ROC's curves and they are displayed. Finally, some conclusions about the results are presented.

## Theoretical foundations

**Definition 1. Hessian Matrix  $2 \times 2$ .** Let  $f = f(x, y)$  a continuous function defined in  $\mathbb{R}^2$ , then, the Hessian matrix of  $f$  denoted by  $\mathcal{H}f(x, y)$ , is defined as a  $2 \times 2$  matrix which groups all the second order derivatives of  $f(x, y)$ :

$$\mathcal{H}f(x, y) = \begin{bmatrix} \frac{\partial^2 f}{\partial x^2} & \frac{\partial^2 f}{\partial x \partial y} \\ \frac{\partial^2 f}{\partial y \partial x} & \frac{\partial^2 f}{\partial y^2} \end{bmatrix}. \quad (1)$$

The method of Frangi works obtaining a vesselness measure of an image, the vesselness is the classification of each bit as a part of a vessel or not. This is achieved using the eigenvalues of the Hessian matrix of the image  $\mathcal{H}I(x, y)$ , and is defined by:

$$\mathcal{H}I = \begin{bmatrix} I_{xx} & I_{xy} \\ I_{yx} & I_{yy} \end{bmatrix}. \quad (2)$$

Where  $I_{xx}$ ,  $I_{xy}$ ,  $I_{yx}$  and  $I_{yy}$  denote the second order derivatives of the intensity image  $I(x, y)$ :

$$\begin{aligned} I_{xx} &= \frac{\partial^2 I}{\partial x^2} = I(x, y) * \sigma^2 G_{xx} \\ I_{yy} &= \frac{\partial^2 I}{\partial y^2} = I(x, y) * \sigma^2 G_{yy} \\ I_{xy} &= \frac{\partial^2 I}{\partial x \partial y} = I(x, y) * \sigma^2 G_{xy} \\ I_{yx} &= I_{xy}. \end{aligned} \quad (3)$$

The symbol \* indicates convolution, in addition,  $G_{xx}$ ,  $G_{xy}$  and  $G_{yy}$  represent the second order of the Gaussian function  $G(x, y)$  defined by:

$$G(x, Y) = \frac{1}{2\pi\sigma^2} \exp\left(-\frac{x^2+y^2}{2\sigma^2}\right), \quad (4)$$

Since  $\mathcal{H}I$  is a symmetrical matrix the eigenvalues  $\lambda_1$  and  $\lambda_2$  are given by:

$$\begin{aligned} \alpha &= \sqrt{(I_{xx} - I_{yy})^2 + 4I_{xy}^2} \\ \lambda_1 &= \frac{I_{xx} + I_{yy} + \alpha}{2} \\ \lambda_2 &= \frac{I_{xx} + I_{yy} - \alpha}{2}, \end{aligned} \quad (5)$$

with the eigenvalues  $\lambda_1$  and  $\lambda_2$  the vesselness measure is calculated with the expression:

$$V_F = \begin{cases} \exp\left(-\frac{R_\beta^2}{2\beta^2}\right) \left[1 - \exp\left(-\frac{s^2}{2\gamma^2}\right)\right], & \text{if } \lambda_1, \lambda_2 > 0 \\ 0, & \text{Otherwise} \end{cases} \quad (6)$$

$R_\beta = \lambda_1/\lambda_2$ ,  $s = \sqrt{\lambda_1 + \lambda_2}$ ,  $\beta = 0.5$ , and  $\gamma$  is defined as a half of the maximum value of  $s$ , the final vesselness image is obtained using different scales for  $\sigma$  for each pixel of the image  $I(x, y)$ .

### Grünwald-Letnikov Fractional derivative

First to all, consider the ratio which define the derivative of a  $f(x)$  function

$$\begin{aligned} f'_r(x) &= \lim_{\Delta x \rightarrow 0} \frac{f(x+\Delta x) - f(x)}{\Delta x} \\ f'_d(x) &= \lim_{\Delta x \rightarrow 0} \frac{f(x) - f(x-\Delta x)}{\Delta x}, \end{aligned} \quad (7)$$

The expressions  $f'_r(x)$  and  $f'_d(x)$  are defined as the forward and backward derivatives. Then, the same process is applied again:

$$f''_d(x) = \lim_{\Delta x \rightarrow 0} \frac{\left[\lim_{\Delta x \rightarrow 0} \frac{f(x) - f(x-\Delta x)}{\Delta x}\right] - \left[\lim_{\Delta x \rightarrow 0} \frac{f(x-\Delta x) - f(x-2\Delta x)}{\Delta x}\right]}{\Delta x} \quad (8)$$

simplifying we have:

$$f''_d(x) = \lim_{\Delta x \rightarrow 0} \frac{f(x) - 2f(x-\Delta x) + f(x-2\Delta x)}{\Delta^2 x} \quad (9)$$

to find the third order derivative the procedure similar:

$$f'''_d(x) = \lim_{\Delta x \rightarrow 0} \frac{1}{\Delta^3 x} [f(x) - 3f(x-\Delta x) + 3f(x-2\Delta x) - f(x-3\Delta x)] \quad (10)$$

since the behavior of the coefficients is binomial, it is easy to find the  $n$ -order derivative using the binomial formula:

$$f_d^{(n)}(x) = \lim_{\Delta x \rightarrow 0} \frac{1}{\Delta^n x} \sum_{k=0}^n (-1)^k \binom{n}{k} f(x - k\Delta x) \quad (11)$$

where  $n \in \mathbb{Z}_+$ , and the binomial coefficient is given by:

$$\binom{n}{k} = \frac{n!}{k!(n-k)!} \quad (12)$$

if,  $n$  is substituted by an arbitrary value  $\alpha \in \mathbb{R}$ , the binomial coefficient is defined by:

$$\binom{\alpha}{k} = \frac{\Gamma(\alpha+1)}{k! \Gamma(\alpha+1-k)}. \quad (13)$$

$\Gamma(\cdot)$  is the gamma function which extends the definition of factorial to arbitrary values.

**Definition 2: Grünwald-Letnikov fractional derivative.** The fractional forward GL derivative is defined as:

$$f_d^{(\alpha)}(x) = \lim_{\Delta x \rightarrow 0} \frac{1}{\Delta^\alpha x} \sum_{k=0}^{\infty} (-1)^k \binom{\alpha}{k} f(x - k\Delta x) \quad (14)$$

and, the fractional backward GL derivative of  $f(x)$  is defined as:

and the backward GL is:

$$f_r^{(\alpha)}(x) = \lim_{\Delta x \rightarrow 0} \frac{1}{\Delta^\alpha x} \sum_{k=0}^{\infty} (-1)^k \binom{\alpha}{k} f(x + k\Delta x) \quad (15)$$

In the case when  $\Delta x = 1$  a simplest version of (14) is obtained

$$D^{(\alpha)}(x) = f(x) - \alpha f(x-1) + \frac{\Gamma(\alpha+1)}{2\Gamma(\alpha-1)} f(x-2) - \frac{\Gamma(\alpha+1)}{3\Gamma(\alpha-2)} f(x-3) + \dots \quad (16)$$

Even though the GL is an old definition, it is very useful in discrete applications, like the image processing, due to its practicality to be implemented in computer systems.

### Enhancing blood vessel using fractional Hessians

In order to apply the fractional derivatives to the algorithm of Frangi a new definition based on Hessian matrixes is necessary.

**Definition 3. Fractional Hessian matrixes**  $2 \times 2$  of order  $1 + \varphi$ , and  $2 + \varphi$ . The fractional Hessian matrix  $2 \times 2$  of the order and  $1 + \varphi$ , where  $\varphi \in (0,1]$  is defined as:

$$\mathcal{H}^{1+\varphi} I = \begin{bmatrix} \frac{\partial^{1+\varphi} I}{\partial x^{1+\varphi}} & \frac{\partial^{1+\varphi} I}{\partial x^\varphi \partial y} \\ \frac{\partial^{1+\varphi} I}{\partial y \partial x^\varphi} & \frac{\partial^{1+\varphi} I}{\partial y^{1+\varphi}} \end{bmatrix} \quad (17)$$

and the fractional Hessian matrix  $2 \times 2$  of order  $2 \leq 1 + \varphi < 3$ , is defined as follows:

$$\mathcal{H}^{2+\varphi} I = \begin{bmatrix} \frac{\partial^{2+\varphi} I}{\partial x^{2+\varphi}} & \frac{\partial^{2+\varphi} I}{\partial x^{1+\varphi} \partial y} \\ \frac{\partial^{2+\varphi} I}{\partial y \partial x^{1+\varphi}} & \frac{\partial^{2+\varphi} I}{\partial y^{2+\varphi}} \end{bmatrix} \quad (18)$$

The proposed method in (Martinez-Jimenez, L. *et Al.* 2018), works using the GL fractional derivative to modifies the Frangi's algorithm creating a fractional Hessian matrix  $\mathcal{H}^\omega I$ , with  $2 \leq \omega < 3$ . The algorithm was probed using an angiogram set of 4 images with its respective ground-truth image, and the area under the ROC's curve. Despite was no probed, was mentioned that the performance of the algorithm decayed when  $\omega < 2$ .

In the present project a similar methodology to (Martinez-Jimenez *et al.* 2018) is implemented, using the GL fractional derivative and the ROC's curve. However, here, a set of 20 angiograms with its respective ground-truth images were utilized. The order of the fractional derivatives was  $\varphi$ ,  $2 \leq \omega < 3$ . Then, the eigenvalues were calculated and with them the vesselness images for each pixel.

### Results

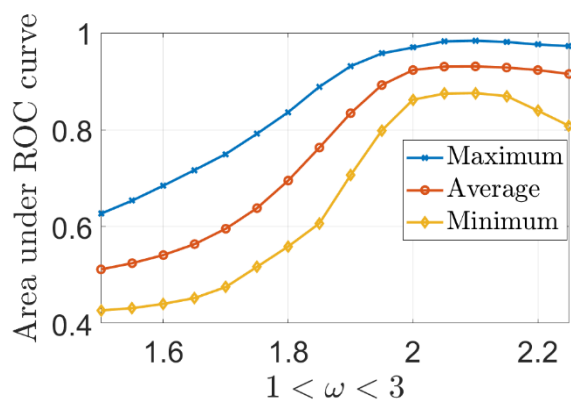
The ROC (*Receiver Operating Characteristic*) is a powerful tool, used to evaluate the performance of a binary classifier. In this case is about the classification the pixels as vessel or not, the results are in the four situations:

- **TP** True positive: A vessel pixel was correctly classified, as a vessel pixel.
- **TN** True Negative: A no vessel pixel was correctly classified as a no vessel pixel.
- **FP** False Positive: A no vessel pixel was incorrectly classified as vessel pixel.
- **FN** False Negative: A vessel pixel was incorrectly classified as no vessel pixel.

The area under the ROC's curve is a graphically way to represent the ratio between the TP against the FP and, the shape of the curve tends to be a rectangle when the total of the TP is near to 100%.

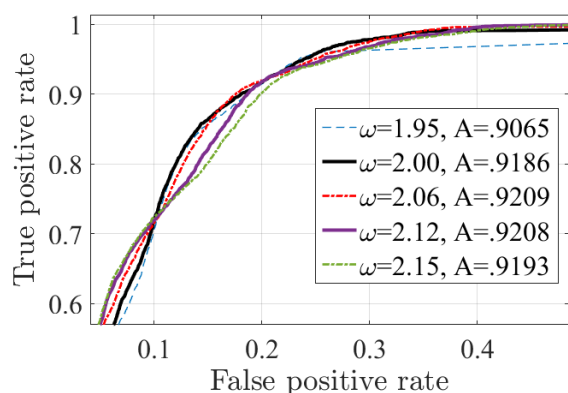
In order to analyze the behavior of the proposed algorithm with fractional orders the study was performed into two steps: in the first one, the algorithm was evaluated using the fractional order in the interval  $1 < \omega \leq 2$ , and in the second the interval was  $2 < \omega < 3$ . Each angiogram image was analyzed using the area under the ROC's curve and each fractional value. With the set of results the mean, the maximum and the minimum for each value of  $\omega$  was calculated. The results are shown in the Plot 1.

Plot 2 shows, the result to apply the algorithm to the angiogram 13, and the fractional orders:  $\omega = 1.95$ ,  $\omega = 2$ , and some values  $\omega > 2$ . We can see that the value of the area is smaller when  $\omega < 0$  than when  $\omega = 0$  and increases as  $\omega > 0$ , however, it reaches its maximum approximately at  $\omega = 2.9$ , after it is decreasing. Specially for  $\omega > 2.13$ .



**Graphic 1** Average, maximum, and minimum values obtained of the set of angiograms and the ROCS's curve, each image was evaluated with fractional orders  $1 < \omega < 3$   
 Source: Own elaboration

The curves show that, using fractional orders  $\omega < 2$ , the area values are smaller than in the ordinary solution ( $\omega = 2$ ), this, confirms that, to use fractional order  $\omega < 2$ , does not improve the results. However, using fractional orders  $\omega > 2$ , help to improve the area values, respect to the ordinary solution, the best results are found when  $2.05 \leq \omega \leq 2.13$ , but the area values decaying with  $\omega > 2.13$ .



**Graphic 2** ROC'S curves using some values of  $\omega$  applied to the angiogram 13 of the set. A is the corresponding area under the curve value  
 Source: Own elaboration

In the Figure 1 the angiogram 13 and its corresponding ground-truth image are shown, in the ground-truth the arteries was marked by a specialist, is utilized as reference to evaluate the performance of the algorithm.

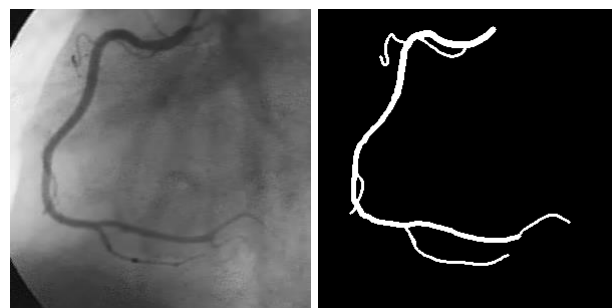


**Figure 1** Angiogram 13 (a) original image and (b) ground-truth image  
 Source: Cervantes-Sanchez et al. 2019

In the Figure 2, the results of apply the algorithm to the angiogram 13 with the fractional orders  $\omega = 1.95$ , and  $\omega = 2.0$  (traditional solution), we can see that, the result when  $\omega = 1.95$  is worse that, the traditional one.

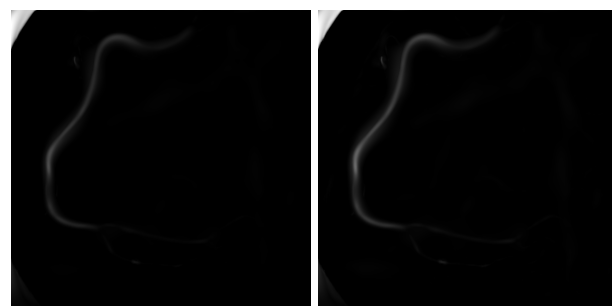


**Figure 2** Obtained result using the algorithm in the angiogram 13, (a) with fractional order  $\omega = 1.95$  and (b) with  $\omega = 2.0$  (traditional solution)  
 Source: Own elaboration

In the Figure 3 the results are shown when the algorithm is applied using the fractional values  $\omega > 2$ , (a) with fractional order  $\omega = 2.06$  and (b) with fractional order  $\omega = 2.09$ , it was the best result.

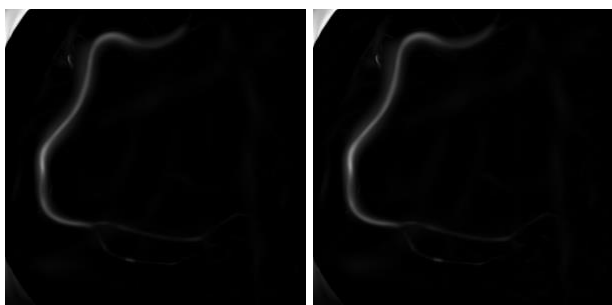


**Figure 3** Obtained result using the algorithm in the angiogram 13, (a) with fractional order  $\omega = 2.06$  and (b) with  $\omega = 2.09$  the best result was obtained here  
 Source: Own elaboration

In the Figure 4 the results are shown when the algorithm is applied using the fractional values  $\omega > 2$ , (a) with fractional order  $\omega = 2.12$  and (b) with fractional order  $\omega = 2.15$ .

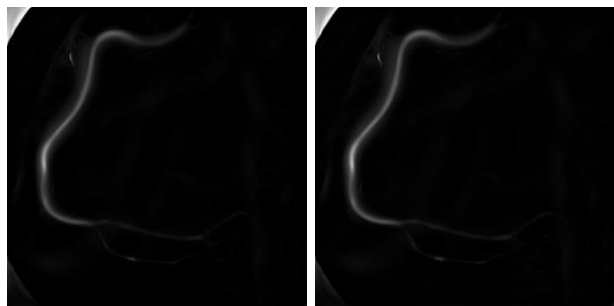


**Figure 4** Obtained results using the algorithm in the angiogram 13, (a) with fractional order  $\omega = 2.12$  and (b) with  $\omega = 2.15$  the best result was obtained here

Source: *Own elaboration*

### Attached

The angiograms database is available in:  
<http://personal.cimat.mx:8181/~ivan.cruz/Databases.html>

### Acknowledgment

The authors wish to thanks to Universidad de Guanajuato, who through DAIP has financed this project with the Institutional Call for Scientific Research 2022 (CIIC2022).

### Conclusions

In this work the proposed algorithm in 2018 based on the Frangi's one and fractional derivatives, was evaluated using fractional orders  $2 < \omega < 3$  and the area under the ROC's curve. The evaluation was using fractional orders in two steps, in the first, the order was in the interval  $1 < \omega < 2$ , and, in the second, was in the interval  $2 < \omega < 3$ . The evaluation of the development of the algorithm was made using 20 angiograms with its respective ground-truth and the ROC's curves. The results show that the best results are obtained when the derivative order is in the interval  $2 < \omega < 2.15$ .

### References

Abel, N. (2012). *Oeuvres complètes de Niels Henrik Abel: Nouvelle édition* (Cambridge Library Collection - Mathematics) (L. Sylow & S. Lie, Eds.). Cambridge: Cambridge University Press. DOI: <https://doi.org/10.1017/CBO9781139245807>.

Abel, N. (2012). *Oeuvres complètes de Niels Henrik Abel: Nouvelle édition* (Cambridge Library Collection - Mathematics) (L. Sylow & S. Lie, Eds.). Cambridge: Cambridge University Press. DOI: <https://doi.org/10.1017/CBO9781139245814>.

Ahmad, B., Batarfi, H., Nieto, J. J., Otero-Zarraquiños, O., and Shammakh W. (2015). Projectile motion via Riemann-Liouville calculus, *Advances in Difference Equations*, 63. DOI: <https://doi.org/10.1186/s13662-015-0400-3>.

Ahmed, A., Nieto J. J., Venkatesh, V. (2015). Fractional Electrical Circuits, *Advances in Mechanical Engineering*, 7(12) 1–7 DOI: <https://doi.org/10.1177/1687814015618127>.

Amoako-Yirenkyi P., Appati J. K., and Dontwi I. K. (2016). A new construction of a fractional derivative mask for image edge analysis based on Riemann-Liouville fractional derivative, *Advances in Difference Equations*, 2016 (238). DOI: <https://doi.org/10.1186/s13662-016-0946-8>.

Angeles Rojas, J. A. (2022). Detección de carcinoma basocelular utilizando red neuronal convolucional y Support Vector Machine. (Bachelor's thesis). Universidad Nacional Mayor de San Marcos. DOI: <https://cybertesis.unmsm.edu.pe/handle/20.500.12672/18365>.

Atangana A., and Baleanu, D. (2016). New fractional derivatives with nonlocal and non-singular kernel: theory and application to heat transfer model. *Thermal Science*, 20(2), 763-769. DOI: [10.2298/TSCI160111018A](https://doi.org/10.2298/TSCI160111018A).

Baskonus, H. M., Mekkaoui T., Hammouch, Z., and Bulut, H. (2015). Active Control of a Chaotic Fractional Order Economic System, *Entropy*. 17, 5771-5783, DOI: [10.3390/e17085771](https://doi.org/10.3390/e17085771). (Haci Mehmet Baskonus, Toufik Mekkaoui, Zakia Hammouch and Hasan Bulut. Active Control of a Chaotic Fractional Order Economic System, *Entropy*. 2015, 17, 5771-5783. DOI: <https://doi.org/10.3390/e17085771>.)

Bouraoui, M., Ronse, C., Baruthio, J., Passat, N., and Germain, P. (2008). Fully Automatic 3D Segmentation of Coronary Arteries Based on Mathematical Morphology. *Proc. 5th IEEE International Symposium on Biomedical Imaging (ISBI 2008): From Nano to Macro*, IEEE, (May 2008), 1059–1062. DOI: [10.1109/ISBI.2008.4541182](https://doi.org/10.1109/ISBI.2008.4541182).

- Capelas de Oliveira, E., and Tenreiro Machado, J., A. (2014). A review of definitions for fractional derivatives and integral. *Mathematical Problems in Engineering*, 2014, 1-6. DOI: <https://doi.org/10.1155/2014/238459>.
- Caputo, M., and Fabrizio, M. (2015). A new Definition of Fractional Derivative without Singular Kernel, *Progr. Fract. Differ. Appl.* 1(2), 73-85. DOI: <http://dx.doi.org/10.12785/pfda/010201>.
- Caputo, M., and Mainardi, F. (1971). A new dissipation model based on memory mechanism. *Pure Appl. Geophys.*, 91, 134-147. DOI: <https://doi.org/10.1007/BF00879562>.
- Cervantes-Sanchez, F., Cruz-Aceves, I., Hernandez-Aguirre, A., Hernandez-Gonzalez, M., A., and Solorio-Meza, S., E. (2019). Automatic Segmentation of Coronary Arteries in X-ray Angiograms using Multiscale Analysis and Artificial Neural Networks. *Applied Sciences* 9(24). 5507. DOI: <https://doi.org/10.3390/app9245507>.
- Chen, W., Sun H., Zhanga, X., and Dean, K. (2010). Anomalous diffusion modeling by fractal and fractional derivatives. *Computers & Mathematics with Applications*, 59(5),1754-1758. DOI: <https://doi.org/10.1016/j.camwa.2009.08.020>.
- Cruz-Aceves, I., and Hernandez-Aguirre A. (2015). Segmentation of Coronary Angiograms Using a Vesselness Measure and Evolutionary Thresholding: Design of Intelligent Systems Based on Fuzzy Logic, Neural Networks and Nature Inspired Optimization, 601. *Series Studies in Computational Intelligence*. 269-289. DOI:10.1007/978-3-319-17747-2\_22.
- Eiho S. and Qian Y. (1997). Detection of coronary artery tree using morphological operator. *Computers in Cardiology*. 24. 525–528. DOI: 10.1109/CIC.1997.647950
- Frangi, A., Niessen. W., Vincken, A., and Viergever, M. (1998). Multiscale Vessel Enhancement Filtering. *Proc. Medical Image Computing and Computer-Assisted Intervention (MICCAI 1998)*. 1496. Springer, 130-137. DOI: <https://doi.org/10.1007/BFb0056195>.
- Guia, M., Gomez, F., and Rosales, J. (2013). Analysis on the time and frequency domain for the RC electric circuit of fractional order. *Open Physics*, 11(10), 1366-1371. DOI: <https://doi.org/10.2478/s11534-013-0236-y>.
- Guzman, D., Roca, S., Pimienta, M., Estrella, C. (2022). Impacto del entrenamiento específico de fuerza muscular sobre los niveles de tensión arterial en adultos mayores con hipertensión arterial: Caso del geriátrico “Cabaña Mis nonos” Guaymallén Mendoza. (Bachelor’s thesis). Universidad Juan Agustín Maza. DOI: <http://repositorio.umaza.edu.ar/handle/00261/2913>.
- Kang, W., Wang, K., Chen, W., and Kang, W. (2009). Segmentation Method Based on Fusion Algorithm for Coronary Angiograms. *Proc. 2nd International Congress on Image and Signal Processing (CISP 2009)*. (Oct. 2009), 1–4. DOI: 10.1109/CISP.2009.5303615.
- Karpinski, K., Sylwia, Zielinska-Raczynska S., and Ziemkiewicz, D. (2021). Fractional Derivative Modification of Drude Model, *Sensors*. 21, 4974. DOI: <https://doi.org/10.3390/s21154974>.
- Khalil, R., Al Horani, M., Yousef, A., and Sababheh A. (2014). A new definition of fractional derivative, *Journal of Computational and Applied Mathematics*, 264 (2014) 65–70. DOI: <https://doi.org/10.1016/j.cam.2014.01.002>.
- Lara, D. S.D., Faria, A. W. C., Araujo, A. A., Menotti, D. (2009). A Semi-Automatic Method for Segmentation of the Coronary Artery Tree from Angiography, *Proc. XXII Brazilian Symposium on Computer Graphics, and Image Processing (SIBGRAPI 2009)*, IEEE. (Oct. 2009), 194–201. DOI: 10.1109/SIBGRAPI.2009.41.
- Maglaveras, N., Haris, K., Efstratiadis, S., Gourassas, J., and Louridas, G. (2001). Artery skeleton extraction using topographic and connected component labeling, *Computers in Cardiology*. 28, 17–20. DOI: 10.1109/ICIP.2001.958497.

Martinez-Jimenez, L., Cruz-Duarte, J. M., Rosales, J. J., and Cruz-Aceves I. (2018). Enhancement of Vessels in Coronary Angiograms Using a Hessian Matrix Based on Grunwald-Letnikov Fractional Derivative. In Proceedings of the 2018 8th International Conference on Biomedical Engineering and Technology (ICBET '18). Association for Computing Machinery, New York, NY, USA, 51–54. DOI: <https://doi.org/10.1145/3208955.3208971>.

Martinez-Jimenez, L., Cruz-Duarte, J. M., Rosales-Garcia, J. J. (2019). Fractional solution of the catenary curve, Math Meth Appl Sci. 1–10. DOI: <https://doi.org/10.1002/mma.5608>.

Martinez-Jimenez, L., Rosales-Garcia, J. J., Ortega-Contreras, A., and Baleanu, D. (2017). Analysis of Drude model using fractional derivatives without singular kernels, Open Phys. 15, 627–636. DOI: <https://doi.org/10.1515/phys-2017-0073>.

Meral, F. C., T.J., Royston T. J., and Magin R. (2010). Fractional calculus in viscoelasticity: An experimental study. Communications in Nonlinear Science and Numerical Simulation, 15(4), 939-945 DOI: <https://doi.org/10.1016/j.cnsns.2009.05.004>.

Navarrete Chiriboga, B. A., and Rivera Guerra, L. M. (2022). Tamizaje cardiológico neonatal por oximetría de pulso como método para la detección temprana de cardiopatías congénitas en el Hospital General Guasmo Sur, servicio de neonatología en el año 2021. (Bachelor's thesis). Universidad Católica de Santiago de Guayaquil. DOI: <http://repositorio.ucsg.edu.ec/handle/3317/18946>.

Schiesselt, H., Metzler, R., Blument, A. and Nonnemacher T. F. (1995). Generalized viscoelastic models: their fractional equations with solutions. Journal of Physics A: Mathematical and General, Gen. 28 6567, 6567-4584. DOI: <https://doi.org/10.1088/0305-4470/28/23/012>.